Control and Synchronization of the Generalized Lorenz System with Mismatched Uncertainties using Backstepping Technique and Time-delay Estimation

Dongwon Kim[1], Maolin Jin[2] and Pyung Hun Chang[3*]

[1]Department of Mechanical Engineering, University of Michigan, Ann Arbor MI 48109

[2]Korea Institute of Robot and Convergence (KIRO), Pohang, Korea

[3]Department of Robotics Engineering, Daegu-Gyeongbuk Institute of Science and Technology (DGIST), Daegu 711-873,
Korea
*Correspondence: phchang@dgist.ac.kr, +82.53.785.6260

Abstract

We propose a robust control technique for regulation and synchronization of the Generalized Lorenz System (GLS) that covers the Lorenz system, Chen system and Lü system. The proposed control provides synergy through the combination of the backstepping control and *time-delay estimation* (TDE) technique. TDE is used to estimate and cancel nonlinearities and uncertainties, and the backstepping method is adopted to provide robustness against matched and mismatched uncertainties. As a result, we observe in numerical simulation that the proposed technique shows better performances in regulating and synchronizing the GLS with mismatched uncertainties, in comparison with existing schemes. The efficacy of the proposed technique is also validated with a circuit-implemented chaotic system.

Keywords: Chaotic system; Robust control; Synchronization; Chaotic circuit; Time-delay estimation; Backstepping.

1. Introduction

Chaotic behaviors provide various applications based on their irregularity and unpredictability. These applications are shown in various fields, including physical, chemical and ecological systems, secure communications [1, 2, 45]. A variety of control theories have been applied to manage chaotic signals [3–12, 30–36]. Recently, for a faster response and enhanced robustness, hybrid methods have appeared in regulating and synchronizing chaotic systems. For example, adaptive control and backstepping technique are combined in [8, 13, 14], optimal control and sliding mode control are used together in [11], fuzzy logic, adaptive control and sliding mode control are merged in [9, 12, 15, 33]. These approaches, however, require a precise chaotic system model, and are vulnerable to parameter variations, modeling errors and external disturbances. Moreover, the hybrid methods are quite complicated.

In 2008, Jin and Chang incorporated the time-delay estimation (TDE) technique to obtain

simplicity and robustness [17]. Jin and Chang's technique comprises three parts: a TDE part to cancel the controlled system's dynamics, an injection part to endow the desired master system's dynamics, and a convergence part to shape the synchronization error dynamics. It provides fast, accurate and robust performance. With the TDE technique, Kim et al. also proposed a regulation and synchronization method using terminal sliding mode (TSM) [18]. Kim's method achieves fast and powerful convergence. The aforementioned two methods based on the TDE technique [17], [18] have no device for suppressing mismatched uncertainties; they are vulnerable to uncertainties that do not satisfy the matching condition.

Suppressing the effect of mismatched uncertainties is important in minimizing the number of control inputs and sensors. In this paper, we propose a simple robust technique that is able to care of mismatched uncertainties in a chaotic system as well as matched uncertainties, through the combination of combine the backstepping technique and TDE technique. The backstepping method enables a systematic and recursive procedure for the design of control laws for systems in strict feedback form, while TDE enables a simple effective compensation for uncertainties. Therefore, the proposed technique provides a single controller that can be applied to any systems in strict feedback form even if a precise system model is not identified. In addition of this benefit, uncertainties that reside on each equation of chaotic systems can be suppressed by TDE conducted on the equation, and all TDE on each equation are governed by the control input. The proposed technique is therefore expected to be superior in dealing with mismatched uncertainties.

To verify the efficacy of the proposed technique, we apply the technique to the regulation and synchronization problems of the Generalized Lorenz System (GLS) introduced in [21, 22]. The GLS covers the well-known classical Lorenz system [23], Chen system [24] and Lü system [25] in one formulation. We perform a comparative study with the TDE-based controllers proposed in previous works [17, 18]. The proposed technique is experimentally validated with a circuit-implemented chaotic system.

This paper is an extension of our previous work originally reported in our short proceeding [1]. In this paper, we additionally provide the stability analysis for the closed-loop system with the proposed technique, and present a real experimental data. Experimental implementation is crucial for practical applications of chaos [11, 26–29] because the signal is always contaminated by noise. Numerical differentiation of state variable is required to implement the proposed technique, and it can easily amplify the noise effect; thus, the proposed technique should be verified through experiment or, at least, computer simulation considering noise. In this paper, we will verify the proposed control through physical chaotic systems with analog circuit elements.

This paper begins with the design procedures of controllers each of which is tailored to the regulation and synchronization problems, respectively, with a brief explanation of the GLS. In the following sections, the proposed controllers are validated through a simulation study and experimental study. We allocate subsections separately to the regulation and synchronization parts as well in these validation studies. Finally, we make remarks in the conclusion section.

2. Controller development

2.1 Regulation

The Generalized Lorenz System (GLS) [2] is described as

$$\dot{\mathbf{x}} = \begin{bmatrix} \mathbf{A} & 0 \\ 0 & \lambda_3 \end{bmatrix} \mathbf{x} + x_1 \begin{bmatrix} 0 & 0 & 0 \\ 0 & 0 & -1 \\ 0 & 1 & 0 \end{bmatrix} \mathbf{x}, \quad \mathbf{A} = \begin{bmatrix} a_{11} & a_{12} \\ a_{21} & a_{22} \end{bmatrix}, \tag{1}$$

where $\mathbf{x} = \begin{bmatrix} x_1 & x_2 & x_3 \end{bmatrix}^T$, $\lambda_3 \in \mathbb{R}$, and matrix $\mathbf{A}$ has eigenvalues $\lambda_1, \lambda_2 \in \mathbb{R}$, $\lambda_{2,3} < 0$, $\lambda_1 > 0$.

The control objective is to regulate $\mathbf{x}$ to a specific constant $\mathbf{x}_d = [x_{1d} \ x_{1d} \ -\frac{x_{1d}^2}{\lambda_3}]^T$. If $x_1(t)$

converges to a specific point x_{1d}, state $x_2(t)$ converges to the specific point x_{1d} as well from the

fact that $\dot{x}_1(t) = 0$. Once $x_1(t)$ and $x_2(t)$ converge to specific a point x_{1d}, state $x_3(t)$ converges

to a certain point based on the characteristic that the parameter (eigenvalue) $\lambda_3 < 0$ (Eq. (1)).

Considering this fact, we can separate the GLS into two parts as follows:

$$\text{First part:} \quad \begin{cases} \dot{x}_1 = a_{11}x_1 + a_{12}x_2 + d_1, \\ \dot{x}_2 = a_{21}x_1 + a_{22}x_2 - x_1x_3 + d_2, \end{cases} \tag{2}$$

$$\text{Second part:} \quad \dot{x}_3 = \lambda_3 x_3 + x_1 x_2,$$

where d_1 and d_2 denote unknown disturbances, which are assumed to be continuous and bounded.

Now, it is required to control the first part of the generalized Lorenz system to achieve the control objective. The control of the first part can be achieved by adding a control input u to the differential equation of state x_2. In order to design a robust backstepping technique, we transform the first part of Eqs. (2) as follows:

$$\begin{cases} \dot{x}_1 = a_{11}x_1 + a_{12}x_2 + d_1, \\ \dot{x}_2 = a_{21}x_1 + a_{22}x_2 - x_1x_3 + d_2 + u, \end{cases} \Rightarrow \begin{cases} \dot{x}_1 = f_1 + g_1 x_2, \\ \dot{x}_2 = f_2 + g_2 u, \end{cases} \Rightarrow \begin{cases} \dot{x}_1 = h_1 + \hat{g}_1 x_2, \\ \dot{x}_2 = h_2 + \hat{g}_2 u, \end{cases} \tag{3}$$

where

$$f_1 = a_{11}x_1 + d_1, \ g_1 = a_{12},$$
$$f_2 = a_{21}x_1 + a_{22}x_2 - x_1x_3 + d_2, \ g_2 = 1, \tag{4}$$

and $h_i (i = 1, 2)$ are terms that include all uncertainties:

$$h_1 = a_{11}x_1 + (a_{12} - \hat{g}_1)x_2 + d_1,$$
$$h_2 = a_{21}x_1 + a_{22}x_2 - x_1x_3 + d_2 + (1 - \hat{g}_2)u, \tag{5}$$

where $\hat{g}_1$ and $\hat{g}_2$ are constants.

With a definition $e_1 \triangleq x_{1d} - x_1$, a Lyapunov function V_1 can be designed as

$$V_1 \triangleq \frac{1}{2}e_1^2. \tag{6}$$

The time derivative of V_1 is

$$\dot{V}_1 = e_1\dot{e}_1 = e_1(\dot{x}_{1d} - h_1 - \hat{g}_1 x_2). \tag{7}$$

From Eq. (7), treating x_2 as a virtual control effort, the 'desired control effort value x_{2d}' for x_2 is chosen so that the negative definiteness of $\dot{V}_1$ is guaranteed.

$$\begin{aligned}
\dot{V}_1 &= -C_1 e_1^2, \\
x_{2d} &\triangleq \hat{g}_1^{-1}(\dot{x}_{1d} + h_1 + C_1 e_1),
\end{aligned} \tag{8}$$

where C_1 is a design parameter.

Since $x_{2d} = \hat{g}_1^{-1}(\dot{x}_{1d} - h_1 + C_1 e_1)$ is a desired control effort and differs from the real state x_2, we denote this 'desired control effort value' as x_{2d}. It is then necessary to find a way to realize x_{2d}. The next step of the backstepping design is to make the error between x_2 and x_{2d} as small as possible.

The actual control effort u is designed so that the error between x_2 and x_{2d} converges to zero. The error between x_2 and x_{2d} is defined as follows:

$$e_2 \triangleq \hat{g}_1(x_{2d} - x_2). \tag{9}$$

We define a Lyapunov function candidate V_2 as

$$V_2 \triangleq \frac{1}{2}e_2^2. \tag{10}$$

Differentiating V_2 with respect to time gives

$$\dot{V}_2 = e_2 \dot{e}_2 = e_2 \hat{g}_1 (\dot{x}_{2d} - \dot{x}_2) = e_2 (\ddot{x}_{1d} - \dot{h}_1 + C_1 \dot{e}_1 - \hat{g}_1 h_2 - \hat{g}_1 \hat{g}_2 u) = -C_2 e_2^2. \tag{11}$$

From Eq. (11), the actual control effort u is chosen so that the negative definiteness of $\dot{V}_2$ is guaranteed.

$$u = (\hat{g}_1 \hat{g}_2)^{-1} (\ddot{x}_{1d} + \hat{g}_1 h_2 + \dot{h}_1 + C_1 \dot{e}_1 + C_2 e_2), \tag{12}$$

where C_2 is a design parameter.

Now, we need to estimate the value of the term $\hat{g}_1 h_2 + \dot{h}_1$. Differentiating the first equation of Eqs. (3) with respect to time gives

$$\ddot{x}_1 = \dot{h}_1 + \hat{g}_1 h_2 + \hat{g}_1 \hat{g}_2 u = H + \bar{B} u, \tag{13}$$

where $H \triangleq \hat{g}_1 h_2 + \dot{h}_1$, $\bar{B} \triangleq \hat{g}_1 \hat{g}_2$.

With the assumption that d_1 and d_2 are continuous, it is reasonable to regard H as a continuous function. It is obvious that the states of GLS are continuous (see Eq. (1)). Then, we could build an approximation $H(t) \cong H(t - L)$, provided that the sampling period L is sufficiently small. This estimation, called TDE [37–44], is formally defined as

$$\hat{H}(t) = H(t - L). \tag{14}$$

For a practical use, the estimate of the term H can be obtained as, using Eq. (13),

$$\hat{H}(t) = H(t - L) = \ddot{x}_1(t - L) - \bar{B}^{-1} u(t - L). \tag{15}$$

TDE is obtained by using the previous-step sensor reading and record of the previous-step input. If the time delay L is sufficiently small, the TDE can estimate and cancel out the system nonlinearities and uncertainties of the system dynamics [37–44]. Therefore, the TDE technique provides simplicity and robustness against uncertainties without substantial computation load. Substituting Eq. (15) into Eq. (12), with the relationship $e_2 = \dot{e}_1 + C_1 e_1$, leads to the final form of the actual control input as follows:

$$u = u(t - L) + \bar{B}^{-1} (\ddot{x}_{1d} - \ddot{x}_1(t - L) + (C_1 + C_2) \dot{e}_1 + C_1 C_2 e_1). \tag{16}$$

The control gains C_1 and C_2 determine how fast the error e_1 converges. In Eq. (16), the delayed acceleration is calculated by numerical differentiation [37–44], as $\ddot{x}_1(t - L) = (x_1(t) - 2x_1(t - L) + x_1(t)) / L^2$.

2.2 Stability Analysis

The stability analysis of the overall closed-loop system is performed and the sufficient condition for closed-loop stability is derived. If the exact value of H was able to be identified, the closed-loop system with the control input would be asymptotically stable, based on the Lyapunov stability theorem. However, since the value of H is estimated using TDE, stability is not guaranteed due to the difference between the real value of H and its estimate. Here, we analyze the stability of the closed-loop system taking the difference into account, grounded on the proof presented in [19].

$$u_{(t)} = \bar{B}^{-1}[v_{(t)} - \hat{H}_{(t)}], \tag{17}$$

where $v_{(t)} \triangleq \ddot{x}_{1d(t)} + (C_1 + C_2)\dot{e}_{1(t)} + C_1 C_2 e_{1(t)}$.

Differentiating the first equation of (3) with respect to time gives

$$\ddot{x}_{1(t)} = H_{(t)} + \bar{B}u_{(t)}. \tag{18}$$

Substituting Eq. (17) into Eq. (18) yields

$$\ddot{x}_{1(t)} - v_{(t)} = H_{(t)} - \hat{H}_{(t)}. \tag{19}$$

With TDE error $\varepsilon_{(t)}$ defined as

$$\varepsilon_{(t)} \triangleq v_{(t)} - \ddot{x}_{1(t)} = \hat{H}_{(t)} - H_{(t)}, \tag{20}$$

we obtain the error dynamics of the proposed control:

$$\ddot{e}_{1(t)} + (C_1 + C_2)\dot{e}_{1(t)} + C_1 C_2 e_{1(t)} = \varepsilon_{(t)}. \tag{21}$$

From the error dynamics, the tracking error $e_{1(t)}$ is influenced by TDE error $\varepsilon_{(t)}$. If $\varepsilon_{(t)}$ is asymptotically bounded, then the error dynamics is also asymptotically bounded [19], and consequently the overall closed-loop system is stable. Therefore, we focus on the boundedness of $\varepsilon_{(t)}$ from now on. To this end, a differential equation representing the dynamics of $\varepsilon_{(t)}$ is derived.

$\ddot{x}_{1(t)}$ in Eq. (3) can be arranged as follows:

$$\ddot{x}_{1(t)} = a_{(t)} + B_{(t)}u_{(t)}, \tag{22}$$

where $B_{(t)} = g_{1(t)}g_{2(t)}, \tag{23}$

$$a_{(t)} = \dot{f}_{1(t)} + \dot{g}_{1(t)} x_{2(t)} + g_{1(t)} f_{2(t)}. \tag{24}$$

The combination of Eq. (18) with Eq. (22) gives

$$H_{(t)} = a_{(t)} + [B_{(t)} - \bar{B}] u_{(t)}. \tag{25}$$

Using Eq. (20), we can arrange Eq. (25) as follows:

$$\varepsilon_{(t)} = H_{(t-L)} - H_{(t)} = a_{(t-L)} + [B_{(t-L)} - \bar{B}] u_{(t-L)} - (a_{(t)} + [B_{(t)} - \bar{B}] u_{(t)}). \tag{26}$$

Substituting Eqs. (15) and (19) into Eq. (26) gives

$$\varepsilon_{(t)} = a_{(t-L)} - a_{(t)} + [B_{(t-L)} - \bar{B}] u_{(t-L)} - [B_{(t)} - \bar{B}][u_{(t-L)} + \bar{B}^{-1}(-\ddot{x}_{1(t-L)} + v_{(t)})]. \tag{27}$$

From the above equations, we derive the following relationships:

$$u_{(t-L)} = \bar{B}^{-1}[\ddot{x}_{(t-L)} - a_{(t)}], \tag{28}$$

and

$$\ddot{x}_{1(t-L)} = a_{(t-L)} - \varepsilon_{(t-L)}. \tag{29}$$

Finally, substituting Eqs. (28) and (29) into Eq. (27) and rearranging it give

$$\varepsilon_{(t)} = [I - B_{(t)}\bar{B}^{-1}]\varepsilon_{(t-L)} + \eta_{1(t-L)} + [I - B_{(t)}\bar{B}^{-1}]\eta_{2(t-L)}, \tag{30}$$

where
$$\eta_{1(t-L)} = [I - B_{(t)}B_{(t-L)}^{-1}][x_{(t-L)}^{(n)} - a_{(t)}] + a_{(t-L)} - a_{(t)}, \tag{31}$$

$$\eta_{2(t-L)} = v_{(t)} - v_{(t-L)}. \tag{32}$$

Taking the same approach presented in [19], the dynamics of $\varepsilon_{(t)}$ in Eq. (30) can be closely approximated by the dynamics behavior of the following sampled-data system (typically, control is carried out in the digital environment):

$$\varepsilon_{(k)} = [I - B_{(k)}\bar{B}^{-1}]\varepsilon_{(k-1)} + \eta_{1(k-1)} + [I - B_{(k)}\bar{B}^{-1}]\eta_{2(k-1)}. \tag{33}$$

Eq. (33) is a first order time-varying difference equation in which $\eta_{1(k-1)}$ and $\eta_{2(k-1)}$, from the viewpoint of $\varepsilon_{(k)}$, are viewed as external inputs acting as disturbances. Next, we establish a sufficient condition for the convergence of $\varepsilon_{(k)}$ based on Eq. (33). We assume that the convergence of $\varepsilon_{(k)}$ implies the convergence of $\varepsilon_{(t)}$ [3]. We further assume that η_1 and η_2 are bounded, and if the eigenvalues

of $I - B_{(k)}\bar{B}^{-1}$ in Eq. (33), denoted by $\xi_{(k)}$, satisfy the condition that $-1 < \xi_{(k)} < 1$, then $\varepsilon_{(k)}$ asymptotically converges to 0. For real systems, $\bar{B}(\triangleq \hat{g}_1 \hat{g}_2)$ is dependent on target system parameters g_1, g_2 that are difficult and time-consuming to estimate exactly. In practice, $\bar{B}^{-1}$ can be tuned without knowledge of the target system. We would recommend starting with a large positive initial value of $\bar{B}^{-1}$ to tune the system performance.

2.3 Synchronization

Synchronization between two chaotic systems is achieved when each state of a slave chaotic system follows its corresponding state of a master chaotic system. Now, we apply the control technique to synchronization between two *identical* chaotic systems with the different initial values using one control input.

The master generalized Lorenz system and slave generalized Lorenz system are given as, respectively,

$$
\begin{aligned}
\dot{x}_{m1} &= a_{11}x_{m1} + a_{12}x_{m2}, \\
\dot{x}_{m2} &= a_{21}x_{m1} + a_{22}x_{m2} - x_{m1}x_{m3}, \\
\dot{x}_{m3} &= \lambda_3 x_{m3} + x_{m1}x_{m2},
\end{aligned}
\tag{34}
$$

$$
\begin{aligned}
\dot{x}_{s1} &= a_{11}x_{s1} + a_{12}x_{s2}, \\
\dot{x}_{s2} &= a_{21}x_{s1} + a_{22}x_{s2} - x_{s1}x_{s3}, \\
\dot{x}_{s3} &= \lambda_3 x_{s3} + x_{s1}x_{s2},
\end{aligned}
\tag{35}
$$

where $\mathbf{x}_m = (x_{m1}, x_{m2}, x_{m3})^T \in R^3$ denotes the state variables of the master system, and $\mathbf{x}_s = (x_{s1}, x_{s2}, x_{s3})^T \in R^3$ denotes the state variables of the slave system.

With the state errors between the slave system and the master system defined as

$$
e_1 \triangleq x_{s1} - x_{m1}, \ e_2 \triangleq x_{s2} - x_{m2}, \ e_3 \triangleq x_{s3} - x_{m3},
\tag{36}
$$

the error system can be derived as

$$
\begin{aligned}
\dot{e}_1 &= a_{11}e_1 - a_{12}e_2, \\
\dot{e}_2 &= a_{21}e_1 + a_{22}e_2 - e_1e_3 - e_1x_{m3} - e_3x_{m1}, \\
\dot{e}_3 &= \lambda_3 e_3 + e_1e_2 + e_1x_{m2} + e_2x_{m1}.
\end{aligned}
\tag{37}
$$

When the error states converge to zero, synchronization between two systems is achieved. Note that the parameter (eigenvalue) λ_3 is below zero. With the fact that the differential equation of the state $e_3(t)$ converges to zero when $e_1(t)$ and $e_2(t)$ converge to zero, the synchronization between two

systems can be achieved by adding a control input to the differential equation of the state e_2. That is, the control input is added to the differential equation of the state x_{s2} of the slave system.

First part:
$$\begin{cases} \dot{e}_1 = a_{11}e_1 - a_{12}e_2, \\ \dot{e}_2 = a_{21}e_1 + a_{22}e_2 - e_1e_3 - e_1x_{m3} - e_3x_{m1} + u, \end{cases} \tag{38}$$
Second part: $\dot{e}_3 = \lambda_3 e_3 + e_1 e_2 + e_1 x_{m2} + e_2 x_{m1}.$

The proposed control can be designed for the first part of Eqs. (38) with the same procedure of regulation in Section 2. The first part can be rewritten as

$$\begin{aligned} \dot{e}_1 &= h_1 + \hat{g}_1 e_2, \\ \dot{e}_2 &= h_2 + \hat{g}_2 u. \end{aligned} \tag{39}$$

The first part is in the same form with Eq. (3). The control input can be derived as follows in the same way proposed in Section 2:

$$u(t) = u(t-L) + \bar{B}^{-1}(\ddot{x}_{m1} - \ddot{x}_1(t-L) + (C_1 + C_2)\dot{e}_1 + C_1C_2e_1). \tag{40}$$

We emphasize that all uncertainty factors in the first part can be dealt with by TDE as long as they are included in h_1 and h_2.

3. Numerical simulation

3.1 Regulation of the Lorenz system

As an example of the generalized Lorenz system to be controlled, the Lorenz system is chosen. The Lorenz system is simple but captures various features of the generalized Lorenz system. To show the robustness of the proposed controller, we take unstructured uncertainties (i.e., disturbances) as well as structured uncertainties (i.e., parameter variations) into account. Bounded continuous disturbances are considered in the differential equations of the state x and state y for more practical circumstances [4]. In addition, the variations of parameters σ, r, and b are also considered. Then, the Lorenz system is described as

$$\begin{aligned} \dot{x} &= (\sigma + \delta\sigma)(y - x) + d_1, \\ \dot{y} &= (r + \delta r)x - y - xz + d_2 + u, \\ \dot{z} &= xy - (b + \delta b)z, \end{aligned} \tag{41}$$

where d_1 and d_2 denote disturbances; u a control input; $\delta\sigma$, δr, δb the corresponding variations

of the parameters $\sigma, r, b,$ respectively.

The parameters of the Lorenz system are selected as $\sigma = 10, r = 28, b = 8/3$. The initial values of each system are set to be $(x_0, y_0, z_0) = (10, 0, -10)$. A fourth-order Runge–Kutta method is used to solve the systems with step size 0.0001 s. Parameter L is set to 0.001 s meaning sampling frequency = 1 kHz in digital implementation. Note that the sampling frequency is sufficiently larger than the Nyquist frequency of the Lorenz system. The design parameters C_1 and C_2 are chosen as 15 to force the error dynamics of the controlled system $\ddot{e}_1 + (C_1 + C_2)\dot{e}_1 + C_1 C_2 e_1 = 0$ to achieve critical damping. The control gain $\bar{B}$ is tuned to 11. The control input is activated at $t= 5$ s and the regulation point is designed as $(x_d, y_d, z_d) = (5,5,9.375),\ \ t \geq 5$ s. The mismatched and matched disturbances are given as $d_1 = \cos(5\pi t)$ and $d_2 = \cos(5\pi t)$. Parameter variations are set to be $\delta\sigma = 0.1, \delta r = 0.2$ and $\delta b = 0.1$, respectively.

The simulation results of the proposed controller are shown in Fig. 1. Figs. 1 (a) and (b) display the time responses of the states of the Lorenz system in the presence of the matched uncertainties alone and in the presence of the matched and mismatched uncertainties. The Lorenz system is regulated to the desired state fast and accurately even under the matched disturbance, mismatched disturbance and parameter variations. Fig. 1 (c) shows the errors between x_d and x during the steady state fall down below ± 0.0006. The steady error improves if the design parameters C_1 and C_2 are set to higher values. To meet the discontinuous shifts of the desired regulation points at $t = 5$ s, the control inputs drastically soar as shown in Fig. 1 (d).

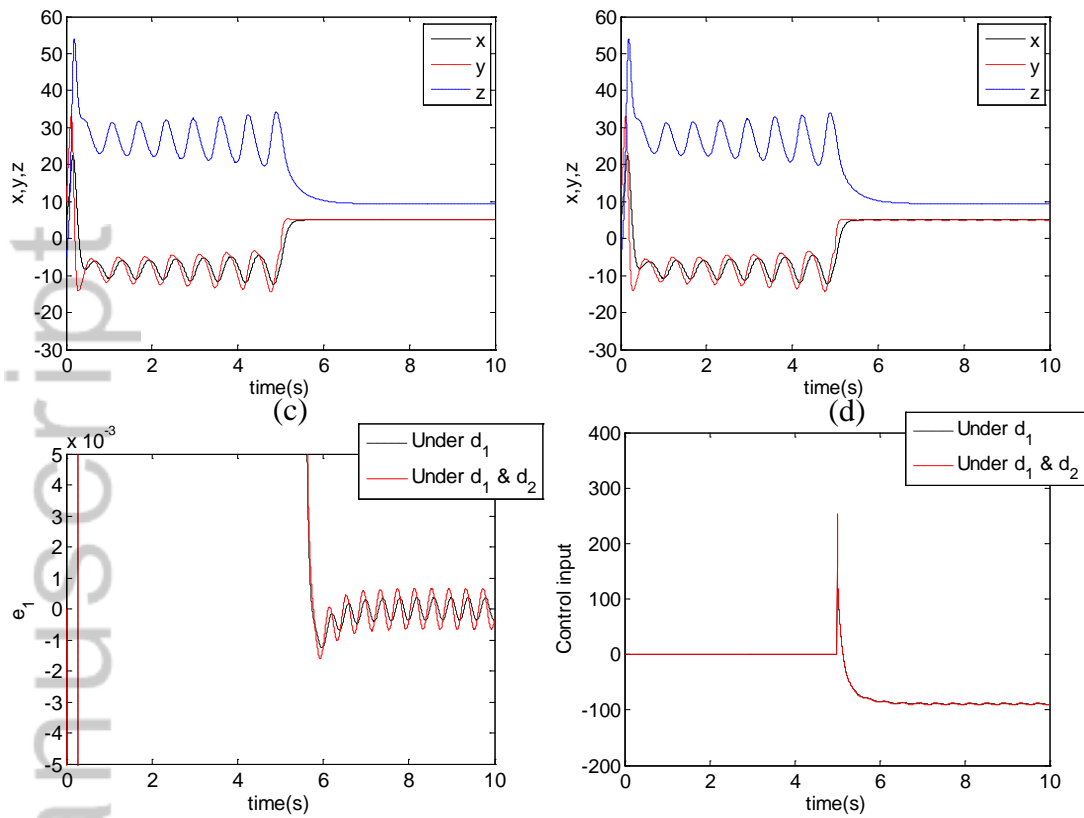(a)   (b)

Fig. 1 Responses of the Lorenz system in the presence of (a) a matched disturbance and (b) matched and mismatched disturbances. The time evolution of (c) error states e_1 and (d) control inputs u for the two cases. The control input is exerted at time 5 s.
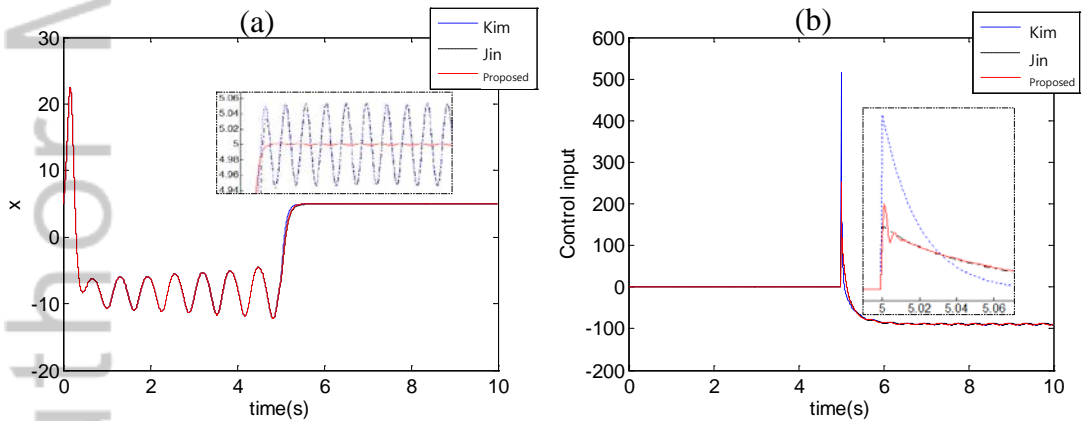

Fig. 2 Time evolution of (a) states x and (b) control inputs u with the controllers proposed in [17] and [18], and with the proposed control. The control input is exerted at time 5 s.

Additionally, we compare the proposed controller with two TDE-based controllers proposed in [17, 18]. The gains are set as $k_1 = 10$, $k_2 = 50$ for Eq. (10) in [17]; $\alpha = 20$, $\beta = 10$, $\gamma = 0.6$ for Eq. (13) in [18]. Both matched and mismatched uncertainties are considered. Fig. 2 shows the responses of the

state x of the Lorenz system and control input u, respectively. The proposed controller shows the smallest steady state error among the three.

The two controllers proposed in [17, 18] use TDE for only the second equation of the controlled system; thus, mismatched uncertainties on the first equation cannot be suppressed. The proposed controller can compensate for the mismatched uncertainties by performing TDE on both the first and second equation.

3.2 Synchronization of the Lorenz systems

The Lorenz system is chosen as an example of the GLS as in the regulation case. The master and slave systems can be expressed as, respectively,

$$(x_m, y_m, z_m): \begin{cases} \dot{x}_m = \sigma(y_m - x_m), \\ \dot{y}_m = rx_m - y_m - x_m z_m, \\ \dot{z}_m = x_m y_m - bz_m, \end{cases} \tag{42}$$

and

$$(x_s, y_s, z_s): \begin{cases} \dot{x}_s = \sigma(y_s - x_s), \\ \dot{y}_s = rx_s - y_s - x_s z_s, \\ \dot{z}_s = x_s y_s - bz_s, \end{cases} \tag{43}$$

where $x_m, y_m, z_m \in \Re$ denote the state variables of the master system; $x_s, y_s, z_s \in \Re$ denote the state variables of the slave system; $\sigma, b, r \in \Re$ are parameters.

The initial values of the master system ((x_m, y_m, z_m) in Eq. (42)) are (x_{m0}, y_{m0}, z_{m0}) = (10, 0, -10). The initial values of the slave system ((x_s, y_s, z_s) in Eq. (43)) to be controlled are set as (x_{s0}, y_{s0}, z_{s0}) = (-10, 0, 10). The state variables of the two Lorenz chaotic systems with the different initial values are shown in Fig. 3. The parameters of both Lorenz systems were selected as $\sigma = 10$, $r = 28$, $b = 8/3$.
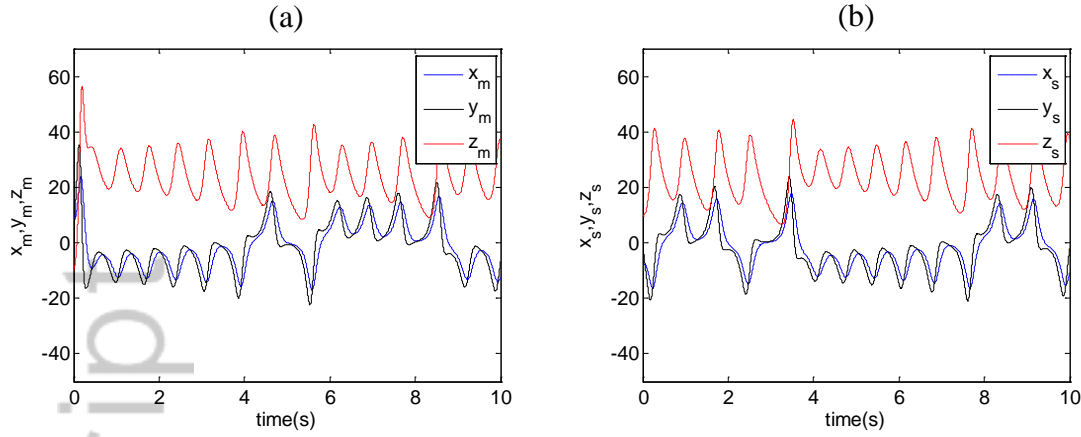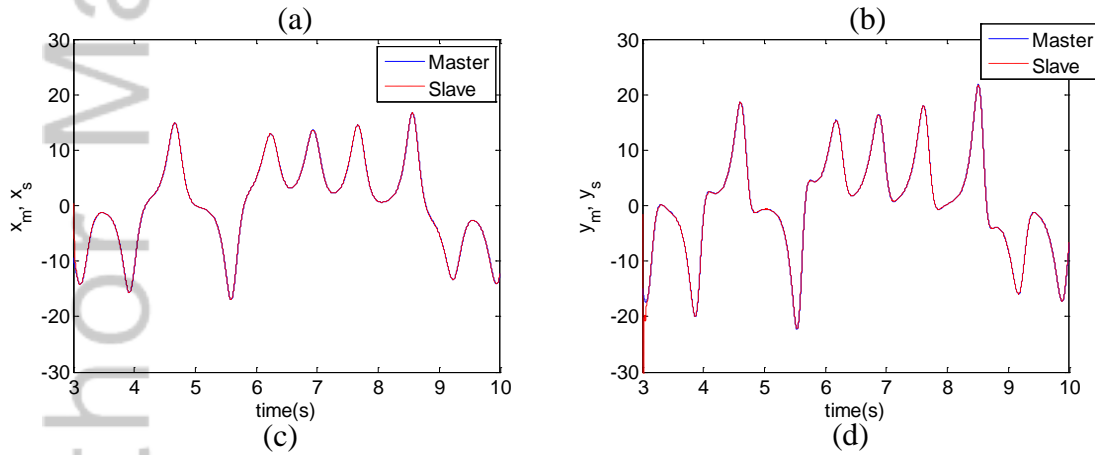
Fig. 3 Time evolution of states of (a) the master Lorenz system and (b) slave Lorenz system.

The error system between the master and slave systems can be written as

$$
\begin{aligned}
&\bullet \begin{bmatrix} \dot{e}_x \\ \dot{e}_y \end{bmatrix} = \begin{bmatrix} \sigma(e_y - e_x) + \delta\sigma(y_s - x_s) \\ re_x - e_y - e_x e_z - e_x z_s - e_z x_s + \delta r x_s \end{bmatrix} + \begin{bmatrix} d_1 \\ d_2 \end{bmatrix} + \begin{bmatrix} 0 \\ 1 \end{bmatrix} u \\
&\bullet \ \dot{e}_z = -be_z + e_x e_y + e_x y_s + e_y x_s - \delta b z_s
\end{aligned}
\tag{44}
$$

where $e_x \triangleq x_m - x_s$, $e_y \triangleq y_m - y_s$, $e_z \triangleq z_m - z_s$.
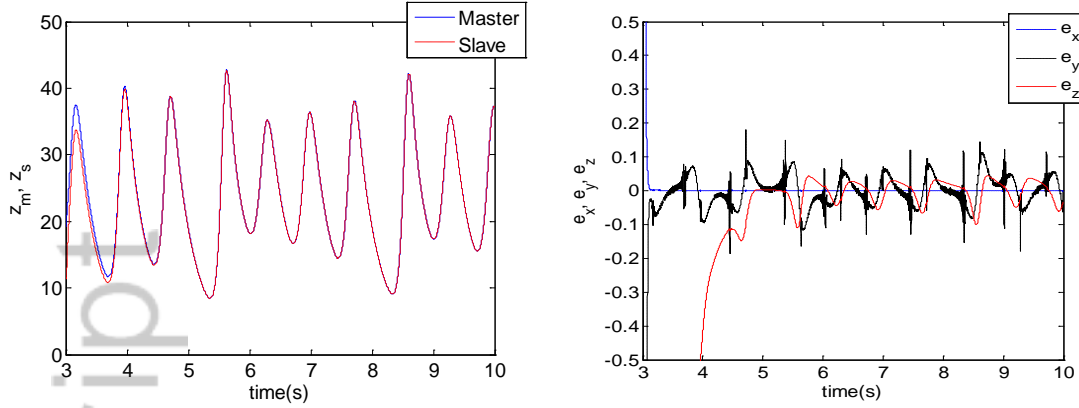
Fig. 4 Time evolution of the master and slave systems: (a) x_m and x_s, (b) y_m and y_s, (c) z_m and z_s. (d) Synchronization errors.

Bounded disturbances and parameter variations are accommodated as shown in Eq. (44). We assume disturbances as $d_1 = \sin(100z)$ and $d_2 = \cos(100x)$. Parameter variations $\delta\sigma$, δr, δb are given as 0.1, 0.2, and 0, respectively. The mismatched parameter variation δb is not considered since it is irrelevant to control performances. Both C_1 and C_2 in Eq. (40) are given as 100 to achieve critical damping when the first error state converses. The larger absolute values of C_1 and C_2 result in the smaller errors. The control input is activated at 3 s, and the control gain $\bar{B}$ is tuned to 50.

The simulation results of synchronization between the two systems are shown in Fig. 4. Fig. 4 exhibits that the state variables of the slave Lorenz system, which is synchronized from $t = 3$ s with the master system. The trajectories of the states of the master system and slave system tightly overlap each other, respectively. The error states converge to zero fast and accurately even under the matched, mismatched disturbances and parameter variations as shown in Fig. 4(d). The control input suddenly fluctuates at $t = 3$ s due to the shifts of the slave system's states toward the desired states at $t = 3$ s.

We have compared the performance of the proposed controller for the synchronization case with that of Kim's controller in [18]. Both of the techniques provide a single controller, which is applied to the second equation of the slave system. The gains are $\alpha = 200$, $\beta = 100$, $\gamma = 0.6$ for Eq. (31) in [18]. Fig. 5 presents the time trajectories of error states and control inputs.

The proposed controller exhibits the better performance in comparison with Kim's controller for error state e_x. This proves the efficacy of the proposed controller in dealing with mismatched uncertainties. Meanwhile, the proposed controller shows the larger synchronization error e_y. This result comes from the fact that the proposed control is originally designed to suppress the first error state, while Kim's controller is designed to suppress only the second error state, assuming that the first and third error equations are internally stable.
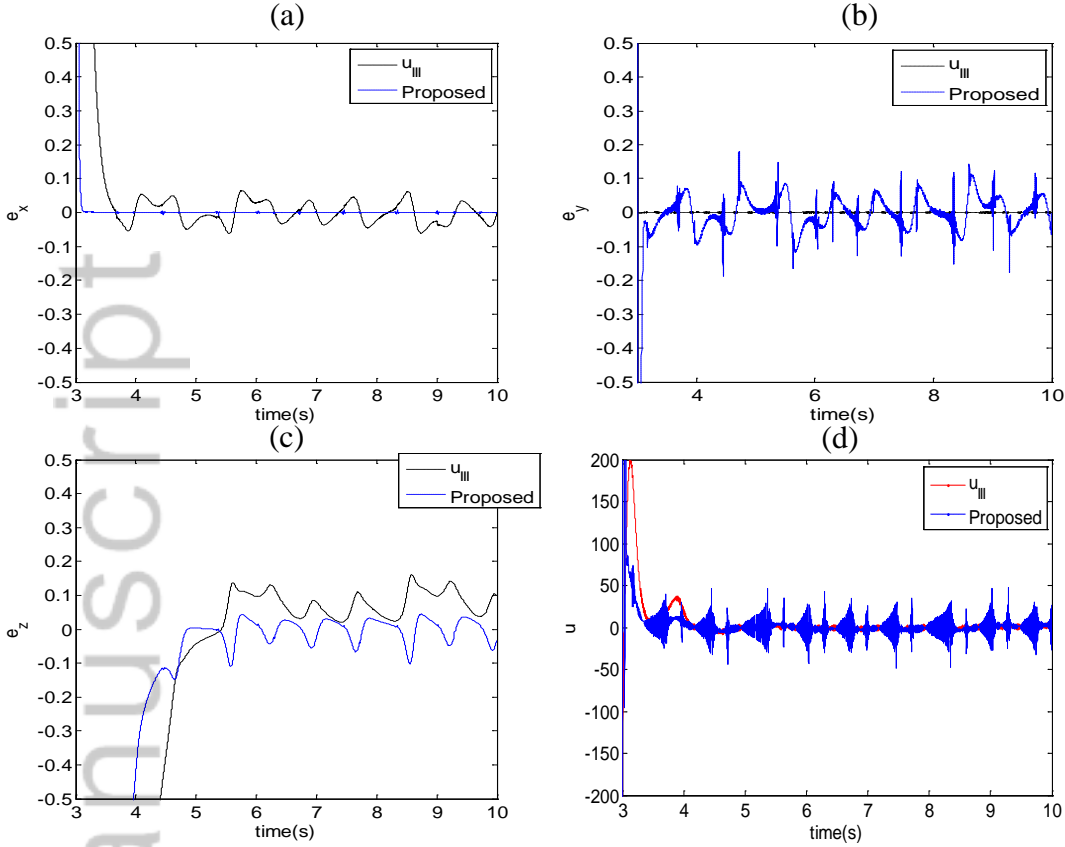
Fig. 5 Time evolution of (a) error state e_x, (b) error state e_y, (c) error state e_z, and (d) control inputs under the control in [18] and the proposed control. The controllers are activated at 3 s.

4. Experiment

4.1 Regulation of the Lorenz system

In this section, we validate the proposed technique in controlling a circuit-implemented chaotic system. The Lorenz system is chosen as an example of the generalized Lorenz system. Considering the fact that the state variables of the system occupy a wide dynamic range with values that exceed the reasonable power supply limits of electric elements, we scale variables in a similar way as proposed in [11].

With the state scaling factors $x' = x/10$, $y' = y/10$, $z' = z/10.$, the Lorenz system is scaled down to

$$
\begin{aligned}
\dot{x}' &= \sigma(y' - x'), \\
\dot{y}' &= rx' - y' - 10x'z', \\
\dot{z}' &= 10x'y' - bz'.
\end{aligned}
\tag{45}
$$

The state variables have similar dynamic ranges and circuit voltages remain well within the range of typical power supply limits. A time scaling factor should be introduced as $t = G_T\tau$, where G_T denotes a time scaling factor. Then, the scaled system is expressed as

$$\dot{x}' = G_T\{\sigma(y' - x')\},$$
$$\dot{y}' = G_T\{rx' - y' - 10x'z'\}, \qquad (46)$$
$$\dot{z}' = G_T\{10x'y' - bz'\}.$$

Four operational amplifiers (LF412, National Semiconductor) and associated circuitry perform operations of sum, multiplication, and integration. Two analog multipliers (AD633, Analog Devices) implement the quadratic terms in the circuit equations. A set of state equations that govern the dynamical behavior of the circuit is obtained as

$$\dot{x}' = \frac{R_5}{C_{p1}}(\frac{1}{R_1}y' - \frac{1}{R_2}x'),$$

$$\dot{y}' = \frac{1}{C_{p2}}(\frac{1}{R_3}x' - \frac{1}{R_5}y' - \frac{1}{10\cdot R_4}x'z'),$$

$$\dot{z}' = \frac{1}{C_{p3}}(\frac{1}{10\cdot R_4}x'y' - \frac{1}{R_7}z').$$

$$\qquad (47)$$

For setting $\sigma = 10$, $r = 28$, $b = 8/3$, the resistors are selected as:
$R_1 = R_2 = 100$, $R_3 = 36$, $R_4 = 10$, $R_5 = 1000$, $R_6 = 10$, $R_7 = 374$ $(k\Omega)$.

The capacitors are selected as
$C_{p1} = C_{p2} = C_{p3} = 47$ (nF).

The Lorenz circuit has a bandwidth of signal x' in about 0 – 120Hz. The time scaling factor G_T of this circuit is estimated as 22. A digital signal processor (DSP, TMS320F2812, Texas Instruments) and TMS320F28X EVM (Texas Instruments) are used for signal processing. Signal conditioning circuits are also considered for ADC input to remain in the range of 0~3V and DAC input to remain in the range of 0~4.096V. A schematic and picture of the experiment settings are shown in Figs. 6 and 7.
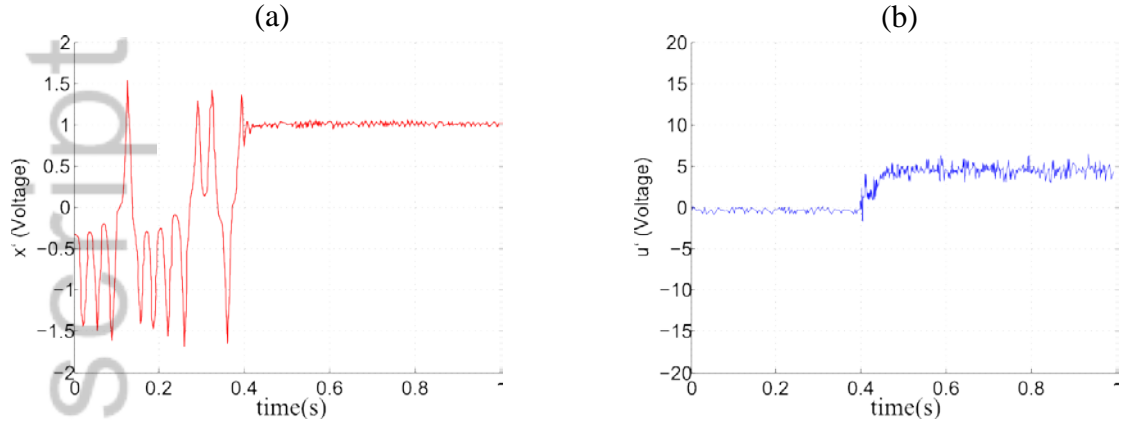
Fig.6 Schematic diagram of control with a DSP EVM.

Fig.7 Overall implementation for control of a chaotic circuit.

The control objective is to regulate x' to 1 V. In the control law (16), the control gain $\bar{B}$ is tuned to 90000, and C_1 and C_2 are both set as 350. The sampling frequency is set as 2 kHz to be sufficiently larger than the Nyquist frequency 240Hz, which is an upper bound on the highest frequency the signal x'.

Figs.8 (a) and (b) show the waveform of the state x' and the corresponding control input u' from the Lorenz circuit, which are measured by an oscilloscope, respectively. The control input is activated at $t = 0.4$. It is observed that the state x' intends to converge to 1V. However, the vibration of the signal x' is displayed during the steady state. The reasons that lead to the vibrations at steady state include unstable power supply to the DSP, ADC resolutions, and the external noise.

Fig.8 Experiment results: time evolution of (a) the state x' and (b) control input u'.

4.2 Synchronization of the Lorenz systems

Next, we conduct synchronization between two identical Lorenz circuits. Firstly, for the control input (40), the gain $\bar{B}$ is tuned to 250000. And, both C_1 and C_2 are set as 550. And the sampling frequency is set as 3.33kHz. The experiment results show that the state x' of the slave system well follows the state x'_d of the master system, as shown in Figs.9 (a) and (b). Fig. 10 displays the control input measured by an oscilloscope.

Uncertainties in the experiments result from external noise, unstable power supply to the DSP, and tolerances of the electronic elements including resistors and capacitors. In particular, in the case of synchronization, the two chaotic circuits are not exactly identical due to the tolerances that give parameter variations. The synchronization error is measured as -33mV ~ 66mV while the magnitude of the desired trajectory rises up to 2.32V. Even in the presence of those uncertainties, we observe that the proposed control achieves synchronization between the two Lorenz circuits.

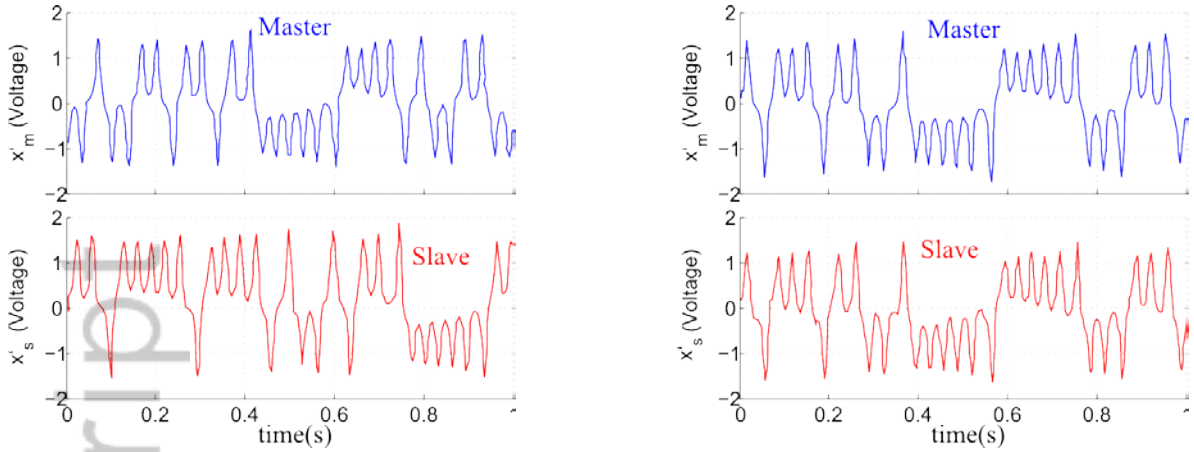(a)   (b)

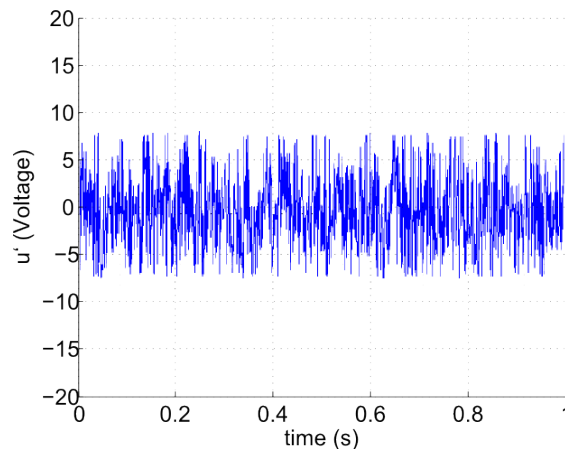**Fig.10** Time evolution of states x'_m and x'_s (a) before and (b) after synchronization.

Fig.11 Time evolution of control input u' for synchronization.

5. Conclusion

We have proposed a robust backstepping technique using time-delay estimation (TDE) to regulate and synchronize the Generalized Lorenz System (GLS) that contains the Lorenz system, Chen system and Lü system. The control technique provides a single controller that can be applied to any chaotic system in strict feedback form for regulation and synchronization, even if a precise model is unavailable. Mismatched uncertainties are managed by multiple TDEs. Numerical simulation results demonstrate fast, accurate and robust performance of the proposed technique in the presence of matched, mismatched disturbances and parameter variations. The proposed technique is experimentally verified with physical chaotic systems constructed by analog circuit elements. The experimental results show satisfactory performances.

References

1. Chen G, Dong X. *From chaos to order: methodologies, perspectives, and applications*. Singapore: World Scientific Pub. Co.; 1998.

2. Andrievskii, B. R., Fradkov A. L. Control of chaos: methods and applications. II. Applications. *Automation and Remote Control* 2004; **65**(4):505–533.

3. Chen C, Chen H. Robust adaptive neural-fuzzy-network control for the synchronization of uncertain chaotic systems. *Nonlinear Analysis: Real World Applications* 2009; **10**(3):1466–1479.

4. Rulkov NF, Tsimring LS. Synchronization methods for communication with chaos over band-limited channels. *International Journal of Circuit Theory and Applications* 1999; **27**(6):555–567.

5. Chen F, Chen L, Zhang W. Stabilization of parameters perturbation chaotic system via adaptive backstepping technique. *Applied Mathematics and Computation* 2008 **200**(1):101–109.

6. Cui F et al. Bifurcation and chaos in the Duffing oscillator with a PID controller. *Nonlinear Dynamics* 1997 **12**(3):251–262.

7. Gambino G, Lombardo MC, Sammartino M. Global linear feedback control for the generalized Lorenz system. *Chaos, Solitons & Fractals* 2006 **29**(4):829–837.

8. Ge SS, Wang C, Lee TH. Adaptive backstepping control of a class of chaotic systems. *International Journal of Bifurcation and Chaos* 2000 **10**(5):1149–1156.

9. Layeghi H et al. Stabilizing periodic orbits of chaotic systems using fuzzy adaptive sliding mode control. *Chaos, Solitons & Fractals* 2008 **37**(4):1125–1135.

10. Liao T, Lin S Adaptive control and synchronization of Lorenz systems *Journal of the Franklin Institute* 1999 **336**(6):925–937.

11. Naseh MR, Haeri M. An optimal approach to synchronize non-identical chaotic circuits: An experimental study. *International Journal of Circuit Theory and Applications* 2011 **39**(9):947–962.

12. Noroozi N, Roopaei M, Jahromi MZ. Adaptive fuzzy sliding mode control scheme for uncertain systems. *Communications in Nonlinear Science and Numerical Simulation* 2009 **14**(11):3978–3992.

13. Yu Y, Zhang S. Adaptive backstepping synchronization of uncertain chaotic system. *Chaos, Solitons & Fractals* 20014 **21**(3):643–649.

14. Wang T et al. Adaptive fuzzy backstepping control for a class of nonlinear systems with sampled and delayed measurements. *IEEE Transactions on Fuzzy Systems* 2015 **23**(2):302–312.

15. Niu Y, Wang X. A novel adaptive fuzzy sliding-mode controller for uncertain chaotic systems. *Nonlinear Dynamics* 2013 **73**(3):1201–1209.

16. Peng C, Chen C. Robust chaotic control of Lorenz system by backstepping design. *Chaos, Solitons & Fractals* 2008 **37**(2):598–608.

17. Jin M, Chang P. Simple robust technique using time delay estimation for the control and synchronization of Lorenz systems. *Chaos, Solitons & Fractals* 2009 **41**(5):2672–2680.

18. Kim D, Gillespie RB, Chang PH. Simple, robust control and synchronization of the Lorenz system. *Nonlinear Dynamics* 2013 **73**(1-2):971–980.

19. Hsia TC, Gao LS Robot manipulator control using decentralized linear time-invariant time-delayed joint controllers. *Proceedings IEEE International Conference on Robotics and Automation*, 1990. 2070–2075.

20. Kim D et al. Control and synchronization of Lorenz systems via robust backstepping technique. *12th International Conference on Control, Automation and Systems (ICCAS)*, 2012. 328–332.

21. Čelikovský S, Vaněček A. Bilinear systems and chaos. *Kybernetika* 1994 **30**(4):403–424.

22. Čelikovský S, Chen G. On a generalized Lorenz canonical form of chaotic systems. *International Journal of Bifurcation and Chaos* 2002 **12**(8):1789–1812.

23. Lorenz EN. Deterministic nonperiodic flow. *Journal of the Atmospheric Sciences* 1963 **20**(2):130–141.

24. Chen G, Ueta T. Yet another chaotic attractor. *International Journal of Bifurcation and Chaos* 1999 **9**(7):1465–1466.

25. Lü J, Chen G. A new chaotic attractor coined. *International Journal of Bifurcation and Chaos* 2002 **12**(3):659–661.

26. Chen D et al. Circuit implementation and model of a new multi-scroll chaotic system. *International Journal of Circuit Theory and Applications* 2014 **42**(4):407–424.

27. Li Y, Tang WKS, Chen G. Hyperchaos evolved from the generalized Lorenz equation. *International Journal of Circuit Theory and Applications* 2005 **33**(4):235–251.

28. Li Y et al. A new hyperchaotic Lorenz-type system: generation, analysis, and implementation. *International Journal of Circuit Theory and Applications* 2011 **39**(8): 865–879.

29. Jafari S, Haeri M, Tavazoei MS. Experimental study of a chaos-based communication system in the presence of unknown transmission delay. *International Journal of Circuit Theory and Applications* 2010; **38**(10):1013–1025.

30. Park C, Lee C, Park M. Design of an adaptive fuzzy model based controller for chaotic dynamics in Lorenz systems with uncertainty. *Information Sciences* 2002 **147**(1): 245–266.

31. Zeng Y, and Singh SN. Adaptive control of chaos in Lorenz system. *Dynamics and*

Control 1997 **7**(2): 143–154.

32. Wu Z et al. Sampled-data fuzzy control of chaotic systems based on a T–S fuzzy model *IEEE Transactions on Fuzzy Systems* 2014 **22**(1):153–163.

33. Zhang L et al. Fuzzy adaptive synchronization of uncertain chaotic systems via delayed feedback control. *Physics Letters A* 2008 **372**(39):6082–6086.

34. Čelikovský S Chen G. On the generalized Lorenz canonical form. *Chaos, Solitons & Fractals* 2005 26(5):1271–1276.

35. Wang Y et al. Adaptive synchronization of GLHS with unknown parameters. *International Journal of Circuit Theory and Applications* 2009 37(8):920–927.

36. Wu X, Cai J, Zhao Y. Some new algebraic criteria for chaos synchronization of Chua's circuits by linear state error feedback control. *International Journal of Circuit Theory and Applications* 2006 34(3):265–280.

37. Youcef-Toumi K, Ito O, A time delay controller for systems with unknown dynamics. *Journal of Dynamic Systems Measurement and Control* 1990 112(1):133–142.

38. Hsia TC, Lasky TA, Guo Z. Robust independent joint controller design for industrial robot manipulators. *IEEE Transactions on Industrial Electronics*, 1991 **38**(1):21–25.

39. Jin M, Lee J, Chang PH, Choi C. Practical nonsingular terminal sliding-mode control of robot manipulators for high-accuracy tracking control. *IEEE Transactions on Industrial Electronics*, 2009 **56**(9):3593–3601.

40. Jin M, Kang SH, Chang PH. Robust compliant motion control of robot with nonlinear friction using time-delay estimation. *IEEE Transactions on Industrial Electronics*, 2008 **55**(1):258–269.

41. Jin M, Lee J, Tsagarakis N. Model-free robust adaptive control of humanoid robots with flexible joints. *IEEE Transactions on Industrial Electronics*, 2017 **64**(2):1706–1715.

42. Lee J, Jin M, Ahn KK. Precise tracking control of shape memory alloy actuator systems using hyperbolic tangential sliding mode control with time delay estimation. *Mechatronics*, 2013 **23**(3):310–317.

43. Jin M, Lee J, Ahn KK. Continuous nonsingular terminal sliding-mode control of shape memory alloy actuators using time delay estimation. IEEE/ASME *Transactions on Mechatronics* 2015 **20**(2):899–909.

44. Jin Y et al. Stability guaranteed time delay control of manipulators using nonlinear damping and terminal sliding mode *IEEE Transactions on Industrial Electronics*, 2013 **60**(8):3304–3317.

45. Wang Q et al. Theoretical Design and FPGA-Based Implementation of Higher-Dimensional Digital Chaotic Systems IEEE Transactions on Circuits and Systems I, 2016 63(3):401–412.
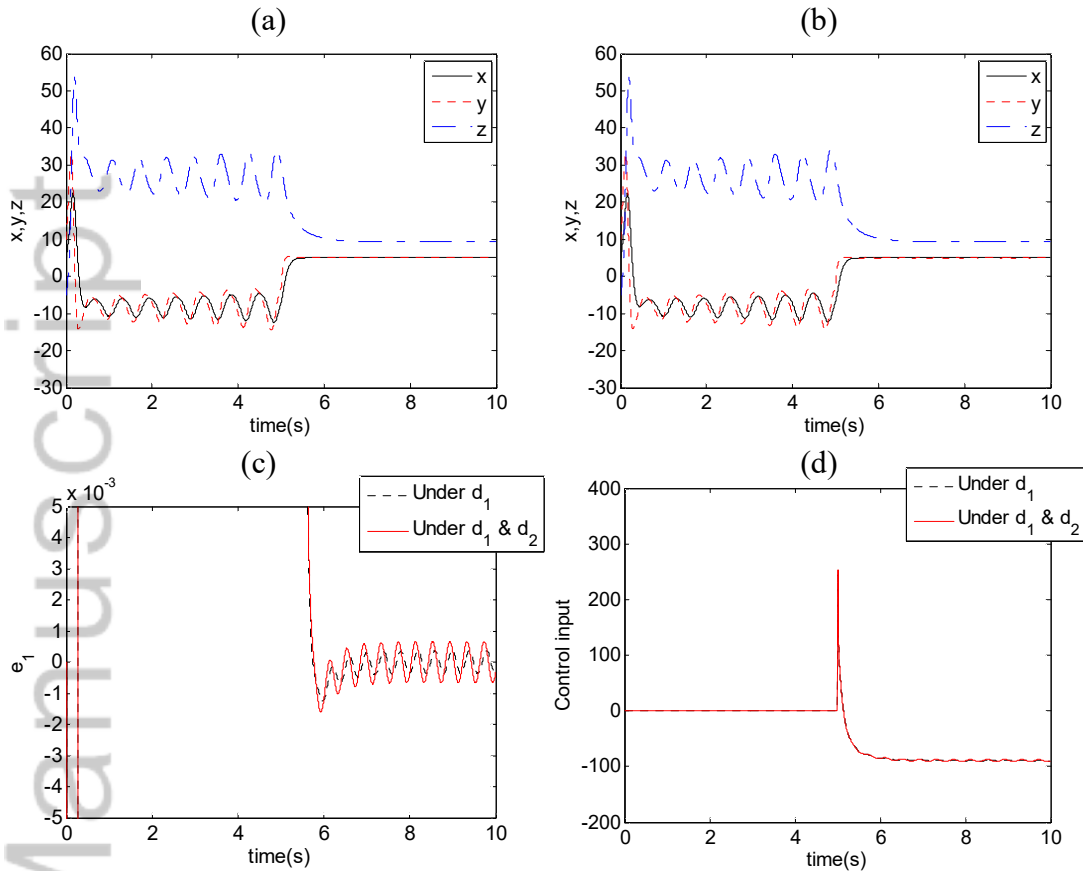
Fig. 1 Responses of the Lorenz system in the presence of (a) a matched disturbance and (b) matched and mismatched disturbances. The time evolution of (c) error states e_1 and (d) control inputs u for the two cases. The control input is exerted at time 5 s.
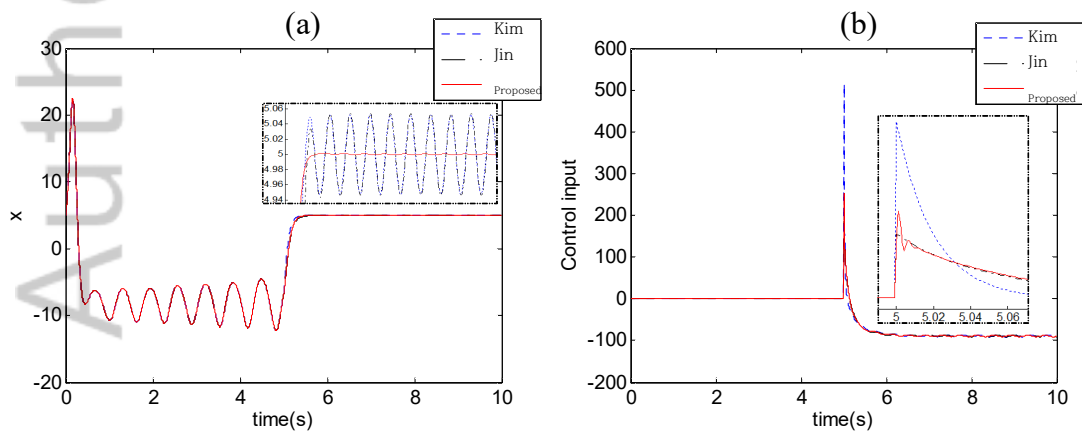

Fig. 2 Time evolution of (a) states x and (b) control inputs u with the controllers proposed in [17] and [18], and with the proposed control. The control input is exerted at time 5 s.
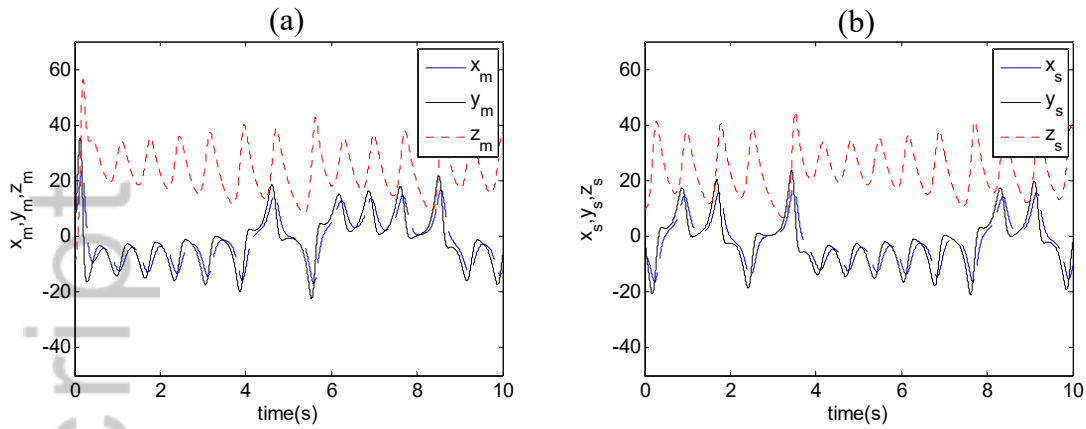
Fig. 3 Time evolution of states of (a) the master Lorenz system and (b) slave Lorenz system.
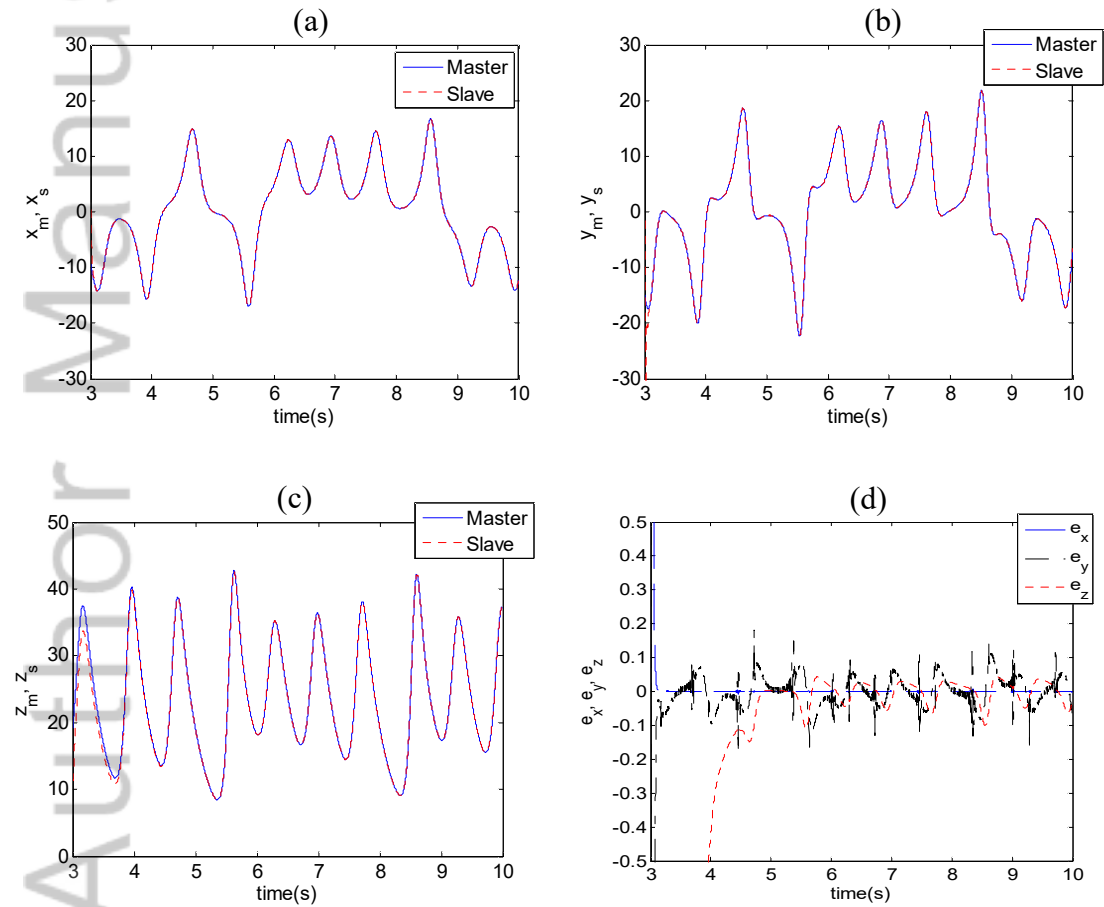
Fig. 4 Time evolution of the master and slave systems: (a) x_m and x_s, (b) y_m and y_s, (c) z_m and z_s. (d) Synchronization errors.
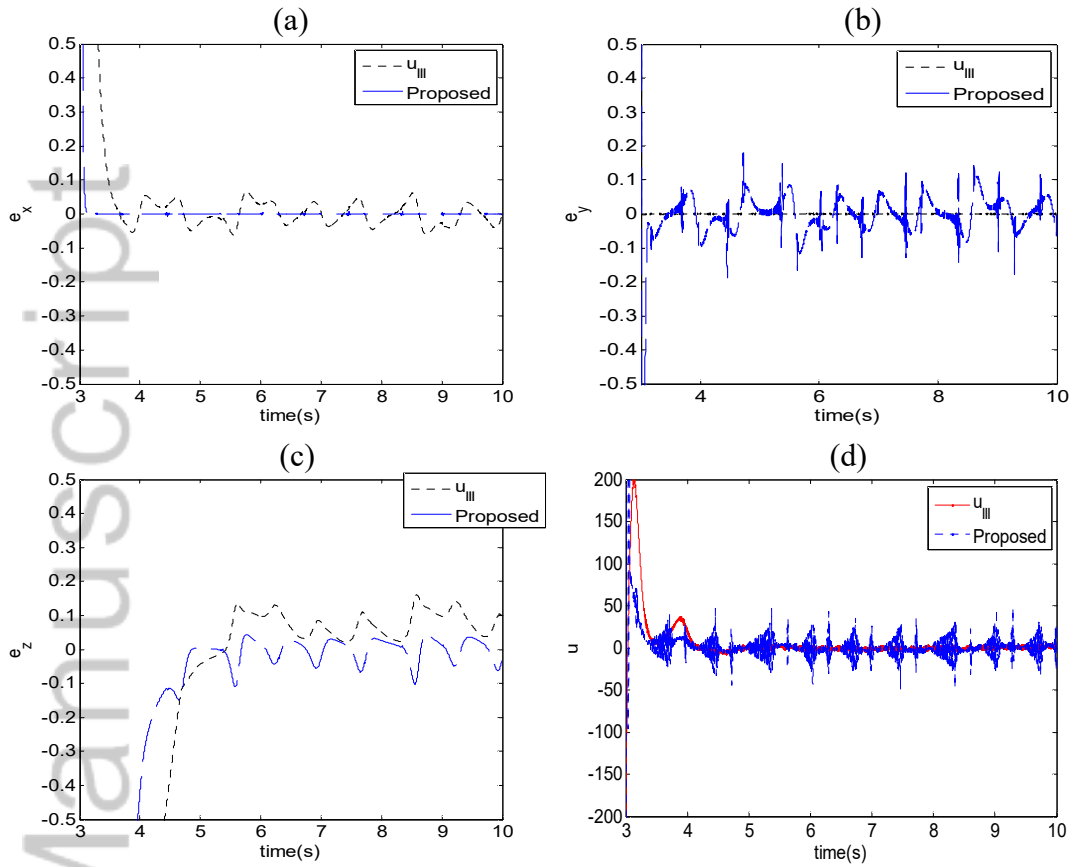
Fig. 5 Time evolution of (a) error state e_x, (b) error state e_y, (c) error state e_z, and (d) control inputs under the control in [18] and the proposed control. The controllers are activated at 3 s.
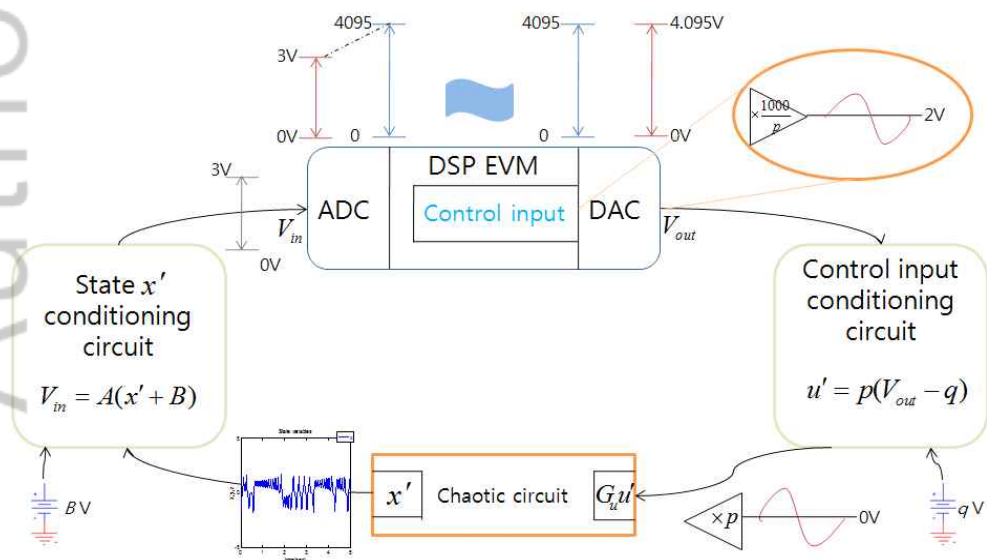

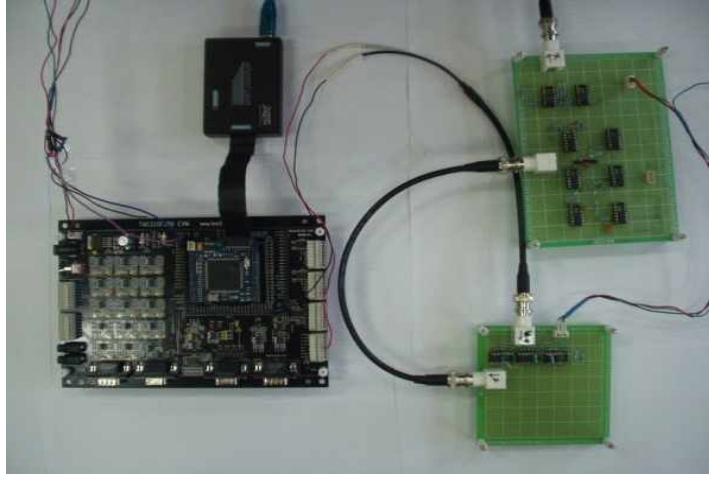**Fig.6** Schematic diagram of control with a DSP EVM.

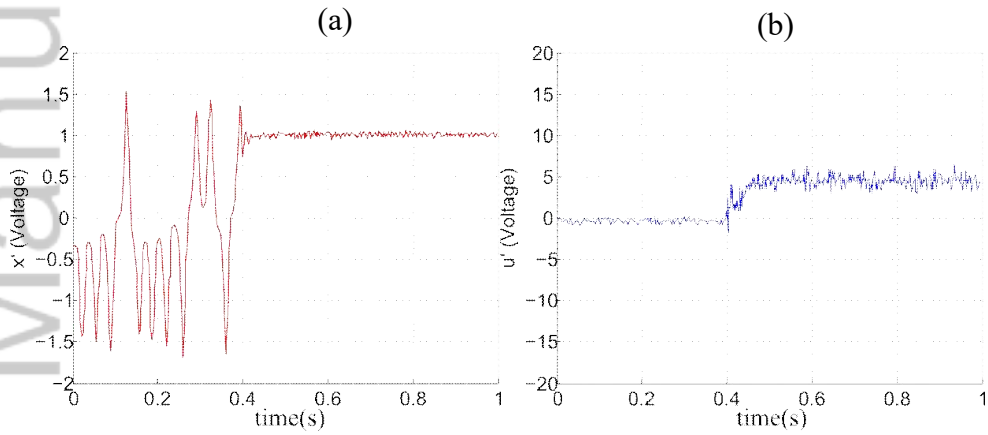**Fig.7** Overall implementation for control of a chaotic circuit.

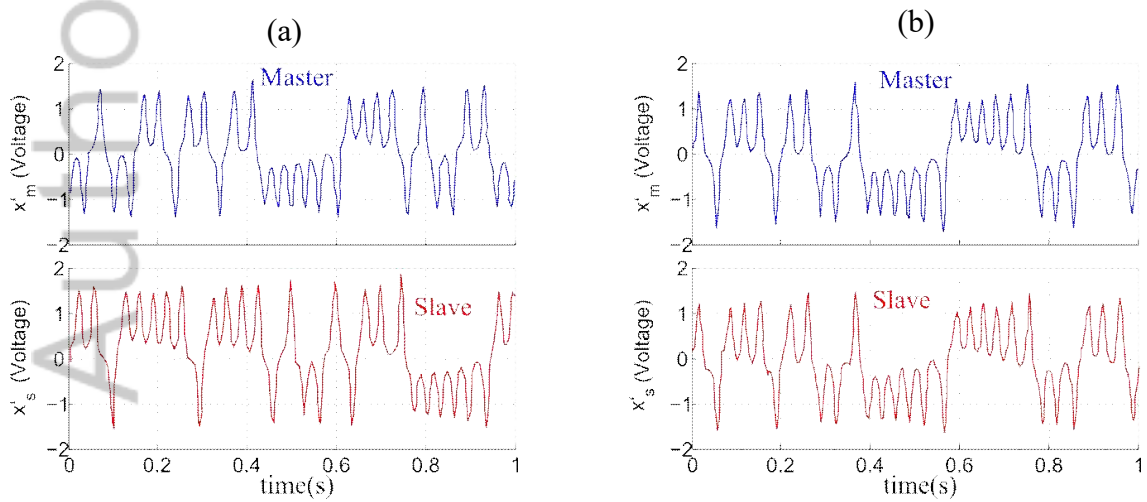**Fig.8** Experimental results: time evolution of (a) state x' and (b) control input u'.

Fig.10 Time evolution of states x'_m and x'_s (a) before synchronization and (b) after synchronization.
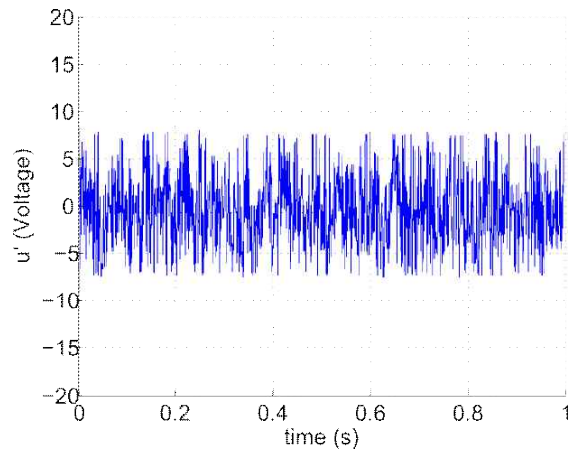
Fig.11 Time evolution of control input u' for synchronization.

The proposed control provides synergy through the combination of the backstepping control and time-delay estimation (TDE) technique. TDE is used to estimate and cancel nonlinearities and uncertainties, and the backstepping method is adopted to provide robustness against matched and mismatched uncertainties.

4095

3V

0V   0

4095   4.095V

0   0V

$\times \dfrac{1000}{p}$ 2V

DSP EVM

3V

ADC   Control input   DAC

V_{in} V_{out}

0V

State x'
conditioning
circuit

$V_{in} = A(x' + B)$

B V

Control input
conditioning
circuit

$u' = p(V_{out} - q)$

State variables

x' Chaotic circuit $G_u u'$

$\times p$ 0V q V